A Network Model for Polarization of Political Opinion

A Network Model for Polarization of Political Opinion

Alex Mantzaris* Desmond J. Higham†

February 3, 2020

Abstract

We propose and study a simple model for the evolution of political opinion through a population. The model includes a nonlinear term that causes individuals with more extreme views to be less receptive to external influence. Such a term was suggested in 1981 by Loren Cobb in the context of a scalar-valued diffusion equation, and recent empirical studies support this modelling assumption. Here, we use the same philosophy in a network-based model. This allows us to incorporate the pattern of pairwise social interactions present in the population. We show that the model can admit two distinct stable steady states. This bi-stability property is seen to support polarization, and can also make the long-term behavior of the system extremely sensitive to the initial conditions and to the precise connectivity structure. Computational results are given to illustrate these effects.

1 Background

There is a rich and growing literature on the design and analysis of models for opinion dynamics. In many application areas, including social science,

*Department of Statistics & Data Science, University of Central Florida, 4000 Central Florida Blvd, Orlando, FL 32816-2370, USA

†School of Mathematics, University of Edinburgh, Edinburgh, EH9 3FD, UK. Supported by grant EP/M00158X/1 from the EPSRC/RCUK Digital Economy Programme and by EPSRC Programme Grant EP/P020720/1. MATLAB code for the computational experiments described here can be found at `https://www.maths.ed.ac.uk/~dhigham/algfiles.html`.

political studies, urban analytics, marketing, and advertising, it is of interest to understand, and possibly to predict and control, how points of view may vary over time in a given population.

Agent-based models motivated by the seminal work of Axelrod [3] represent one important modeling approach. Our work is closer in spirit to the network-based setting used by DeGroot [8], Friedkin & Johnsen [9], and Hegselmann & Krause [16], where a link between a pair of individuals represents an opportunity for influence. Here, opinions propagate iteratively, with each individual taking account of the views of their immediate neighbors. We refer to [1, 2, 5, 10, 15] for details about the current state of the art.

Our aim in this work is to show that the addition of an appropriate nonlinearity in a simple network-based model can lead to subtle effects that, in particular, may lead to a polarization of opinions across the population. The nonlinear term is motivated by the work of Cobb [7], who developed a political opinion model in a stochastic differential equation setting. Cobb introduced the nonlinearity on the basis of a hypothesis that extreme views are more engrained—if we move towards the ends of the political spectrum then we take less notice of external influences.

We note that since Cobb's original work, researchers in the social sciences have developed theories of *unthinking or confident extremists* [6] and *rigidity-of-the-extreme* [19] that support the basic modeling assumption. In particular, empirical tests suggest that "extremists were less influenced than political moderates by two types of experimenter-generated anchors" [6], and "strong partisan intensity predicts reduced cognitive flexibility, regardless of the political party's orientation and doctrine" [19].

The main contributions of our work are

- to develop a network-based model that incorporates a Cobb-style nonlinearity,
- to derive analytical results that show how the nonlinearity can produce polarized populations,
- to perform computational experiments that illustrate how the model behaves on realistic network structures.

The manuscript is organized as follows. In section 2 we describe the original Cobb model from [7]. The new model, which applies when pairwise connectivity information is available, is introduced Section 3. Uniform

steady states of the model are studied analytically and computationally in section 4, with particular attention paid to the case of a periodic ring connectivity structure. In section 5 we then describe further simulations where the topology is based on samples from random network models. We finish with some conclusions in section 6.

2 Cobb Model

In [7], Cobb proposed a simple stochastic differential equation (SDE) model for the dynamics of political opinion. To describe the model, we let the scalar-valued stochastic process $x(t)$ denote the political opinion of an individual at time t. Here, $0 \leq x(t) \leq 1$, with 0 and 1 representing the extreme ends of a one-dimensional spectrum. To be concrete, we will arbitrarily regard $x(t) = 0$ and $x(t) = 1$ as extremely "liberal" and extremely "conservative" convictions, respectively. Cobb suggested that $x(t)$ should satisfy the SDE[1]

$$dx(t) = r\,(\theta - x(t))\,dt + \epsilon\sqrt{x(t)(1-x(t))}dW(t), \tag{1}$$

where $W(t)$ represents standard Brownian motion, and the equation is to be interpreted in Ito form [11, 13]. The model (1) involves three constants. The value $0 < \theta < 1$ represents the "average" or "typical" long-term opinion, and the value $r > 0$ controls the rate at which the long-term expected value is approached. More precisely, letting $\mathbb{E}[\cdot]$ denote the expected value operation, we have $\mathbb{E}[x(t)] - \theta = (\mathbb{E}[x(0)] - \theta)\,e^{-rt}$. The diffusion coefficient $\epsilon\sqrt{x(t)(1-x(t))}$ in (1) quantifies the random fluctuations that an individual's political opinions may undergo. The factor $\sqrt{x(t)(1-x(t))}$ causes these fluctuations to be smallest for people who hold extreme views. Hence, Cobb's model is built on the assumption that *people closer to the ends of the political spectrum have opinions that are more strongly engrained*. The parameter ϵ, which, without loss of generality, may be taken to be non-negative, controls the overall strength of these random fluctuations; ϵ will be large in a population undergoing political unrest, and small in a tranquil population.

We note that the diffusion term in (1) also appears in the classical Fisher-Wright model in population genetics [12].

[1] In this work, we find it natural to use ϵ for the parameter that takes the form ϵ^2 in [7]. Also, since we will be using capitals to denote matrices, we use θ rather than G for the long-time mean.

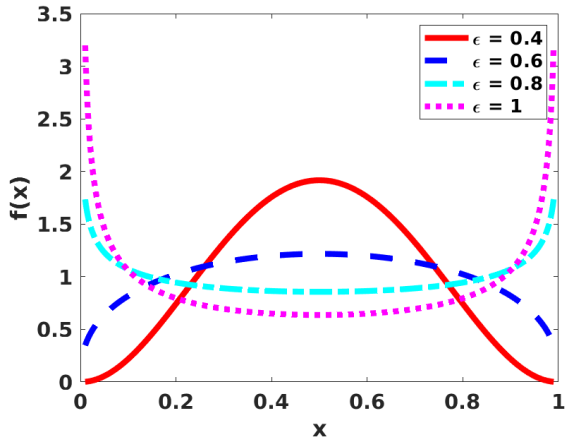

Figure 1: The beta density function (2) for fixed values $r = 1$ and $\theta = \frac{1}{2}$ and four different ϵ values: $\epsilon = 0.4, 0.6, 0.8$ and 1.

Cobb focussed on the long-time, or steady state, distribution of $x(t)$ and solved the associated steady Fokker-Planck equation to give

$$f(x) = \frac{\Gamma(1/\delta)}{\Gamma(\theta/\delta)\Gamma((1-\theta)/\delta)} x^{-1+\theta/\delta}(1-x)^{-1+(1-\theta)/\delta}, \tag{2}$$

as the density function over $(0, 1)$, where $\delta = \epsilon^2/r$. Here $\Gamma(\cdot)$ in (2) denotes the Gamma function, and $f(x)$ is the density function for a Beta distribution with shape parameters θ/δ and $(1-\theta)/\delta$. Cobb's key observation was that the steady state density changes qualitatively as the model parameters are varied. In particular, for a given mean value θ and attraction rate r, increasing the fluctuation strength ϵ can switch the steady state from a unimodal to U-shaped; i.e., *in a time of unrest, political consensus may break down, leading to a polarization of opinions.*

Figure 1 illustrates this effect. Here we superimpose the beta density function (2) with fixed values $r = 1$ and $\theta = \frac{1}{2}$ for four different ϵ values: $\epsilon = 0.4, 0.6, 0.8$ and 1. In this case, the exponents of x and $(1-x)$ in (2) are both $1 - 1/(2\delta)$. These exponents switch from positive to negative as ϵ increases beyond $1/\sqrt{2} \approx 0.7071$.

3 New Network Model

Our aim now is to develop a network-based model that builds on the ideas of Cobb. We start with the assumption that the random fluctuations in (1) are driven by exposure to new ideas, which itself derives from interactions with other members of the population. We may then move to a microscale model, which simultaneously tracks the trajectory of each individual, based on the assumptions that

1. each individual, if left alone, would have an opinion that reverted to the value θ,

2. the current opinion of each individual is also affected by the current opinions of their associates,

3. an individual who currently holds an extreme view is less likely to be affected by their associates than an individual who currently holds a more moderate view.

To produce a model, we assume that there are n individuals whose associations are represented by a fixed adjacency matrix $A \in \mathbb{R}^{n\times n}$. So $a_{ij} = 1$ if person i has the potential to be influenced by person j, and $a_{ij} = 0$ otherwise. By construction $a_{ii} = 0$. Note that A is not required to be symmetric. Let d_i denote the number of influencers of person i; in graph-theoretical terms, d_i is the out-degree of node i. We will work with the scaled adjacency matrix $\widehat{A}$, which has ij entry given by a_{ij}/d_i. Hence, $\widehat{A}$ has all row-sums equal to one.

We will develop the model over discrete time, with integer time points $k = 0, 1, 2, \ldots$, letting $\mathbf{u}^k \in \mathbb{R}^n$ be such that u_i^k is the opinion of person i at time point k. Our model then takes the form

$$\mathbf{u}^{k+1} = F(\mathbf{u}^k), \tag{3}$$

where $F : \mathbb{R}^n \to \mathbb{R}^n$ satisfies

$$(F(u))_i = u_i + r(\theta - u_i) + \epsilon u_i(1 - u_i)\left((\widehat{A}u)_i - \theta\right), \quad \text{for } 1 \le i \le n. \tag{4}$$

Here, as in the original Cobb model (1), the parameter $r > 0$ determines the rate at which an isolated individual would approach the level θ and $\epsilon > 0$ controls the strength of the external influence. However, rather than

having a general diffusion term, this network-based model takes account of the local interactions; the factor $(\widehat{A}u)_i - \theta$ takes the average view over the network neighbors and compares this with the value θ. If this average over the neighbors exceeds θ, then, on the grounds that node i is associating with a group whose views are currently more conservative than the typical value θ, the term $\epsilon u_i(1-u_i)\left((\widehat{A}u)_i - \theta\right)$ makes a positive contribution to u_i^{k+1} in (3). Conversely, if the average opinion over the neighbours is below θ, then this term reduces u_i^{k+1} in (3).

4 Uniform Steady States

To get some insight into the model (3) we look for *uniform* steady states; that is, time-invariant solutions of the form $\mathbf{u}^k = u^\star \mathbf{1}$, for some real-valued scalar $u^\star$, where $\mathbf{1} \in \mathbb{R}^n$ has all components equal to one. Imposing $u^\star \mathbf{1} = F\left(u^\star \mathbf{1}\right)$ in (3), and using $\widehat{A}\mathbf{1} = \mathbf{1}$, we arrive at the scalar equation

$$r(\theta - u^\star) + \epsilon u^\star (1-u^\star)(u^\star - \theta) = 0.$$

This has solutions when $u^\star = \theta$ and when $u^\star$ solves the quadratic equation

$$u^2 - u + r/\epsilon = 0. \tag{5}$$

The quadratic (5) has solutions

$$u_{1,2} = \tfrac{1}{2} \pm \tfrac{1}{2}\sqrt{1 - 4r/\epsilon}.$$

We require these roots to be real and to lie between zero and one. This restricts us to

$$\frac{r}{\epsilon} \leq \frac{1}{4}. \tag{6}$$

As $r/\epsilon \to 0$ from above, these roots tend to 0 and 1. As $r/\epsilon \to 1/4$ from below, the roots both tend to $1/2$.

To understand the relevance of these fixed points, we now consider their linear stability. We mention first the special case where $\epsilon = 0$. In this case (3) corresponds to n independent copies of the scalar recurrence $u^{k+1} = f(u^k)$, where $f(u) = u + r(\theta - u)$. This has a single fixed point at $u = \theta$, which is linearly stable when $|f'(\theta)| < 1$; that is $|1 - r| < 1$, which becomes $r < 2$. *It makes sense to restrict our attention to the case where in the absence of*

external influence an individual naturally evolves to the steady state value θ; so henceforth we impose $r < 2$.

For a general fixed point of the map (3), linear stability is characterized by the Jacobian of F having spectral radius less than one. Basic calculus shows that this Jacobian has the form

$$\frac{\partial F}{\partial u} = (1-r)I + \epsilon \operatorname{diag}\left[(1-2u_i)\left((\widehat{A}u)_i - \theta\right)\right] + \epsilon \operatorname{diag}\left[u_i(1-u_i)\right]\widehat{A}. \quad (7)$$

Here, for $v \in \mathbb{R}^n$, we are using $\operatorname{diag}[v_i]$ to denote the diagonal matrix

$$\begin{bmatrix} v_1 & & & \\ & v_2 & & \\ & & \ddots & \\ & & & v_n \end{bmatrix} \in \mathbb{R}^{n\times n}.$$

We may now evaluate the Jacobian at the uniform fixed points. For $\mathbf{u}^\star = \theta\mathbf{1}$ we find that

$$\frac{\partial F}{\partial u} = (1-r)I + \epsilon\theta(1-\theta)\widehat{A}. \quad (8)$$

Then for $\mathbf{u}^\star = u^\star\mathbf{1}$ with $u^\star = u_1$ or $u^\star = u_2\mathbf{1}$ we have

$$\frac{\partial F}{\partial u} = \left(1 - r + \epsilon(1-2u^\star)\left(u^\star - \theta\right)\right)I + r\widehat{A}. \quad (9)$$

The expressions (8) and (9) lead to the following conclusions concerning the linear stability of the uniform fixed points in terms of the model parameters.

- The steady state $\mathbf{u}^\star = \theta\mathbf{1}$ is linearly stable when

$$|(1-r) + \epsilon\theta(1-\theta)\lambda_i| < 1, \quad (10)$$

  for every eigenvalue λ_i of $\widehat{A}$.

- The steady state $\mathbf{u}^\star = u_1\mathbf{1}$ is linearly stable when

$$\left|\left(1 - r + \epsilon(1-2u_1)\left(u_1 - \theta\right)\right)I + r\lambda_i\right| < 1 \quad (11)$$

  for every eigenvalue λ_i of $\widehat{A}$. Similarly for $\mathbf{u}^\star = u_2\mathbf{1}$.

4.1 Analysis for the Periodic Ring with $\theta = \frac{1}{2}$

We now focus on the simple case of a nearest neighbour periodic ring, where

$$\widehat{A} = \tfrac{1}{2} \begin{bmatrix} & 1 & & & 1 \\ 1 & & 1 & & \\ & \ddots & & \ddots & \\ & & 1 & & 1 \\ 1 & & & 1 & \end{bmatrix} \in \mathbb{R}^{n \times n}. \tag{12}$$

The ring with $n = 10$ nodes is illustrated in Figure 2. Here, each node is connected to its nearest neighbors on the periodic one-dimensional lattice. The network is undirected, so $\widehat{A}$ is symmetric and hence has real eigenvalues. The eigenvalues of $\widehat{A}$ are known to be

$$\lambda_i = \cos(2\pi k/n), \quad \text{for } 1 \le k \le n.$$

So the most positive eigenvalue is 1 and the most negative eigenvalue is -1 when n is even and $\cos(\pi(n+1)/n)$ when n is odd, which is $-1 + O(n^{-2})$. We will assume that n is even to avoid this slight complication.

We also assume for simplicity that $\theta = \frac{1}{2}$.

For the steady state $\mathbf{u}^\star = \frac{1}{2}\mathbf{1}$, at the extreme of $\lambda = 1$ in (10) we obtain

$$-8 + 4r < \epsilon < 4r.$$

At the extreme of $\lambda = -1$, we obtain

$$8 - 4r > \epsilon > -4r.$$

Together, these reduce to the following stability constraint for the steady state $\mathbf{u}^\star = \frac{1}{2}\mathbf{1}$:

$$\epsilon < 4 \min(r, 2 - r). \tag{13}$$

(Recall that we are assuming $r < 2$.) So we have $\mathbf{u}^\star = \frac{1}{2}\mathbf{1}$ stable if the diffusion coefficient ϵ is not too big.

For the other two possible uniform steady states, we note that for $u^\star = u_1$ or $u^\star = u_2$ and $\theta = \frac{1}{2}$ we have $u^\star - \theta = (2u^\star - 1)/2$. So

$$(1 - 2u^\star)(u^\star - \theta) = -\frac{(1 - 2u^\star)^2}{2}. \tag{14}$$

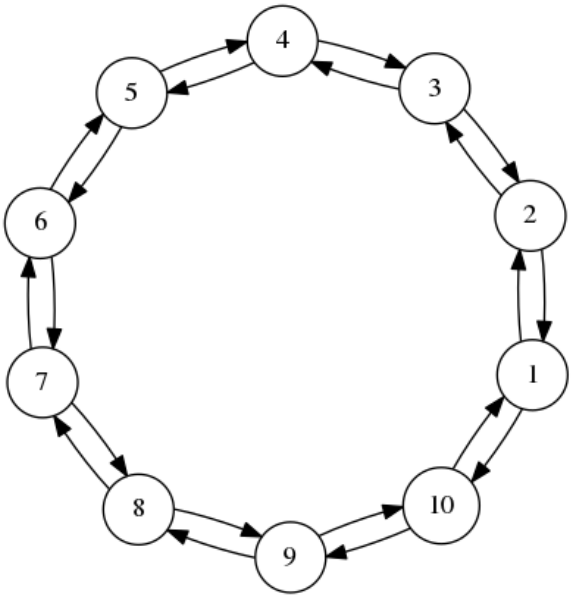

Figure 2: An illustration of the periodic ring in the case of $n = 10$ nodes.

Since $1 - 2u^\star = \pm\sqrt{1 - 4r/\epsilon}$, this gives, in (14),

$$(1 - 2u^\star)(u^\star - \theta) = -\frac{(1 - 4r/\epsilon)}{2} = \frac{-1}{2} + \frac{2r}{\epsilon}. \tag{15}$$

We need to impose (11) with the extreme eigenvalues of $\lambda = 1$ and $\lambda = -1$. For $\lambda = 1$, using (15) we require

$$-1 < 1 - r + \epsilon\left(\frac{-1}{2} + \frac{2r}{\epsilon}\right) + r < 1.$$

This simplifies to $-2 < 2r - \epsilon/2 < 0$. Only one of these is active (because $4r < \epsilon$ is being assumed, from (6)), so we require $\epsilon < 4(r + 1)$.

For $\lambda = -1$, using (15) we require

$$-1 < 1 - r + \epsilon\left(\frac{-1}{2} + \frac{2r}{\epsilon}\right) - r < 1.$$

This simplifies to $-2 < -\epsilon/2 < 0$. Only one of these is active (because $\epsilon > 0$), so we require $\epsilon < 4$.

Overall, we find that $\epsilon < 4$ is the constraint that determines linear stability of the fixed points $\mathbf{u}^\star = u_1\mathbf{1}$ or $\mathbf{u}^\star = u_2\mathbf{1}$.

In summary, in this idealized case we find that

- in order for the steady states $\mathbf{u}^\star = u_1\mathbf{1}$ or $\mathbf{u}^\star = u_2\mathbf{1}$ to exist and have linear stability, we require $r < 1$, in which case they exist and are stable for $4r < \epsilon < 4$,
- in this case, where $r < 1$, the steady state $\mathbf{u}^\star = \frac{1}{2}\mathbf{1}$ is stable for $\epsilon < 4r$.

This scenario corresponds to the classic supercritical pitchfork bifurcation and period doubling cascade seen for the logistic map [14]; the two new steady states emerge when the original steady state becomes unstable. Figure 3 plots the size of these fixed points in a bifurcation diagram, with dashed lines denoting instability. We note that the new model captures the underlying effect of the SDE (1): *increasing the diffusion coefficient can cause the θ-level consensus to break down allowing more extreme views to be supported.*

4.2 Simulations for the Periodic Ring with $\theta = \frac{1}{2}$

To illustrate the relevance of the analysis in subsection 4.1, we show a simulation result. Here, we used $\theta = \frac{1}{2}$, $r = \frac{1}{2}$ and $\epsilon = 2.5$, with a population of size $n = 32$. In this case the $\mathbf{u}^\star = \frac{1}{2}\mathbf{1}$ steady state is unstable and the two states $\mathbf{u}^\star = u_1\mathbf{1}$ and $\mathbf{u}^\star = u_2\mathbf{1}$ with $u_1 \approx 0.2764$ and $u_2 \approx 0.7236$ are stable.

To perform the simulation, we needed to make a decision about how to deal with values of u_i^k that leave the interval $[0, 1]$. We chose to set $u_i^{k+1} = 0$ and $u_i^{k+1} = 1$ if the map (4) produced $u_i^{k+1} < 0$ or $u_i^{k+1} > 1$, respectively.

We set the initial condition to be $u_i^0 = 0.3+0.225v_i$, where $v_i = \exp(y_i)/(1+\exp(y_i))$ and the components y_i run over 32 equally spaced values between -10 and 10. This shifted and scaled sigmoid function was chosen so that one subset of the initial population has views close to the lower value u_1 and another subset has views close to the higher value u_2.

Figure 4 shows the evolution of $\mathbf{u}^k$. We see that there is an initial phase where one set of connected nodes is drawn towards u_1 and another is drawn towards u_2. So both stable steady states are relevant for these intermediate dynamics. Of course, it is not possible for the whole solution to consist of a combination of these two distinct steady state values, and after around 200 time steps the lower steady state at u_1 is seen to dominate—the entire

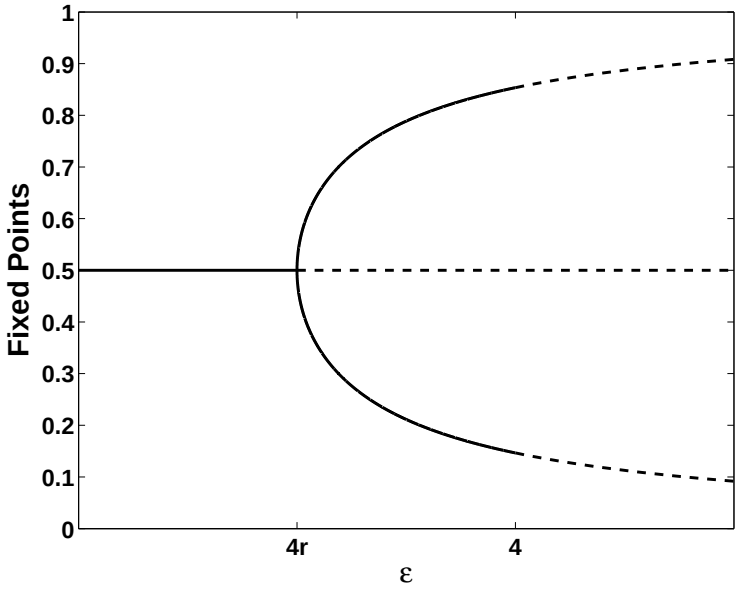

Figure 3: Bifurcation diagram for spatially uniform fixed points on a periodic ring when $\theta = \frac{1}{2}$, in terms of ϵ, with fixed $r < 1$. Vertical axis represents size of components in the spatially uniform fixed point.

population has been attracted to this value. For further clarification, Figure 5 plots the profile of the solution after 0, 150 and 300 timesteps.

Further experiments with larger values of n indicate that is possible for the system to spend a long time in a region where the majority of the nodes can be split into two groups, with one group close to u_1 and the other to u_2. Indeed, such a polarized solution can effectively act as a fixed point in floating point arithmetic. In Figure 6, we repeat the computation from Figure 4 with n increased to 100. Here, the numerical solution is such that the relative Euclidean norm difference between successive iterates, $\| \mathbf{u}^{k+1} - \mathbf{u}^k \|_2 / \| \mathbf{u}^k \|_2$, falls to the level of unit roundoff: it reached $\approx 3.7 \times 10^{-16}$ after 200 steps in a computation using IEEE double precision. Thereafter it remained constant over time to within floating point accuracy.

In Figure 7 we use same parameters as in Figure 6 with a different initial condition. Here, we draw each u_i^0 independently from the uniform $(0.4, 0.6)$ distribution, which is symmetric about the unstable fixed point $u^\star = \frac{1}{2}$. In this case, we see that isolated pockets emerge around the u_1 and u_2 levels, some of which merge at the expense of others. After around 320 steps the solution settled to a profile that remained almost constant (the relative normwise change over each step was less than 2×10^{-7}) for a much longer computation of $10,000$ steps. The profile of this solution is shown in Figure 8; the effect of the two stable steady states is apparent.

5 Random Network Structure

5.1 Rewiring the Ring

The classical "small world" model of Watts and Strogatz [18] uses a parametrized rewiring process to interpolate between a periodic lattice and a fully random graph. Motivated by that work, we now look at the effect of rewiring the periodic ring network in subsection 4.2. For a given probability p, the rewiring process has the following form. Here, we regard each undirected edge as a separate pair of directed edges.

1 Loop over every edge in the original network (that is, every nonzero entry in A).

2 For each edge, $i \to j$, with independent probability p, replace the index j by an index chosen uniformly at random from the full set $1, 2, \ldots, n$.

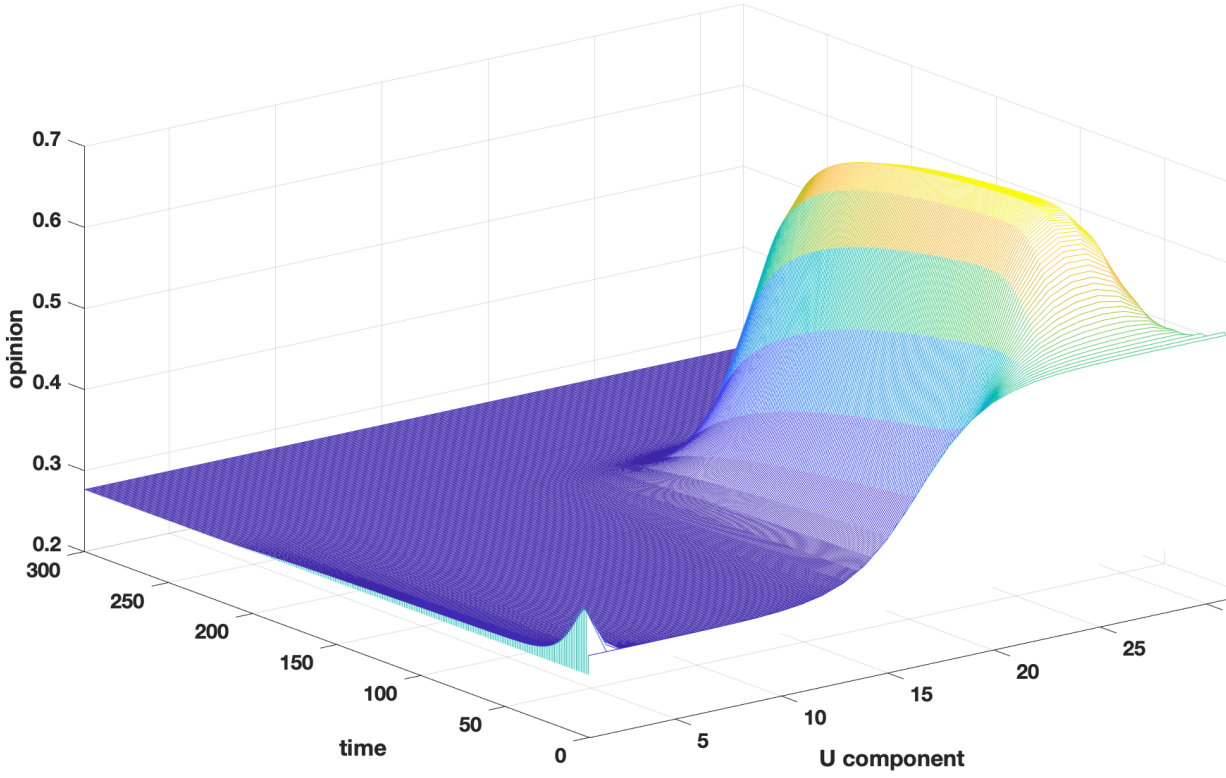

Figure 4: Evolution of opinions when there are two extreme stable steady states in the map (4) for a periodic ring. Here, and throughout all experiments, $\theta = \frac{1}{2}$, $r = \frac{1}{2}$ and $\epsilon = 2.5$, giving $u_1 \approx 0.2764$ and $u_2 \approx 0.7236$. For this test we have $n = 32$ nodes.

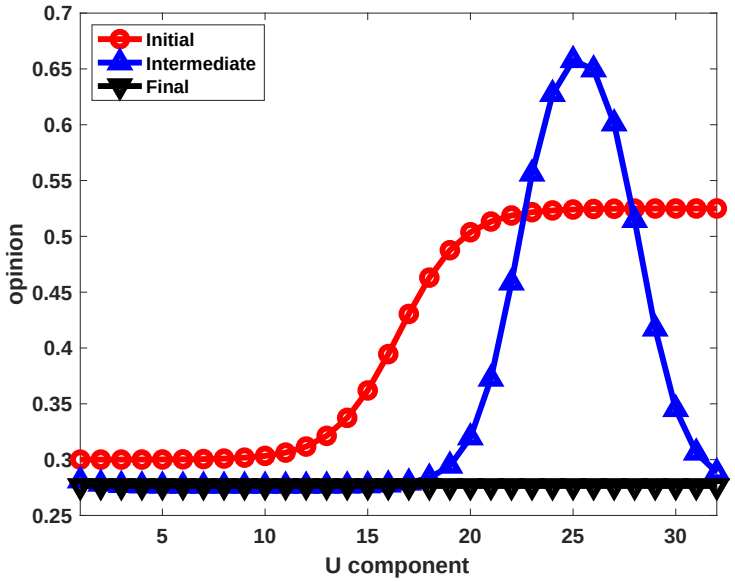

Figure 5: Opinion profiles from Figure 4 at initial, intermediate and long times.

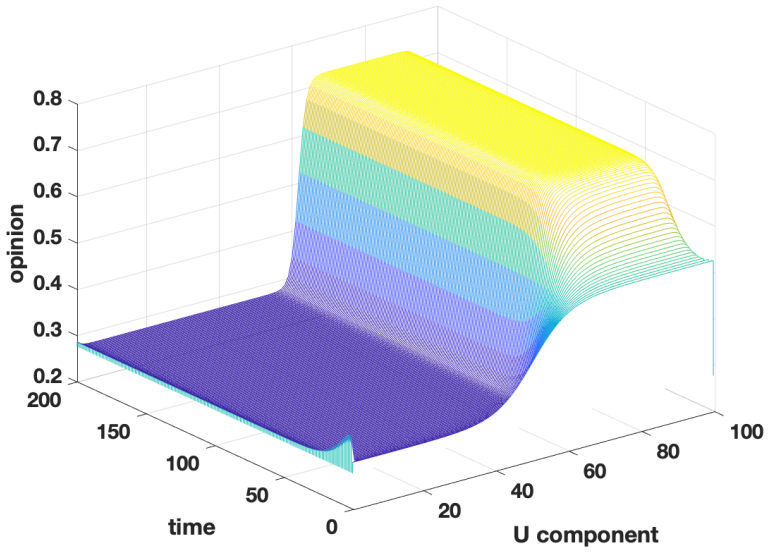

Figure 6: As in Figure 4 with number of nodes increased to $n = 100$.

For Figure 9 we used the same model parameters and initial condition as in Figure 6, but with A arising from a rewired ring with $p = 0.1$. Here, rewiring 10% of the edges has broken up the lattice structure, so that the smooth initial condition no longer maps onto definite neighbors. We see that a much more fragmented transient phase arises than that in Figure 6, before the u_2 state eventually dominates. Figure 10 repeats the computation with a different random number seed, so that the microscale detail of the wiring is changed. In this case the long term solution is attracted to u_1. So we see that, because the underlying deterministic system is bi-stable, the long term dynamics can be dependent upon the very fine scale structure of the random rewiring.

In Figure 11 we look at the effect of the rewiring probability p on two quantities. The plot on the left shows an approximation of the mean time to reach a numerical steady state. More precisely, for each fixed p in a range between 0.1 and 0.9, we simulated with 10^4 independently sampled rewirings, using the same parameters and initial condition as in Figure 6. The vertical axis in the plot represents the sample average of k = final, where final is

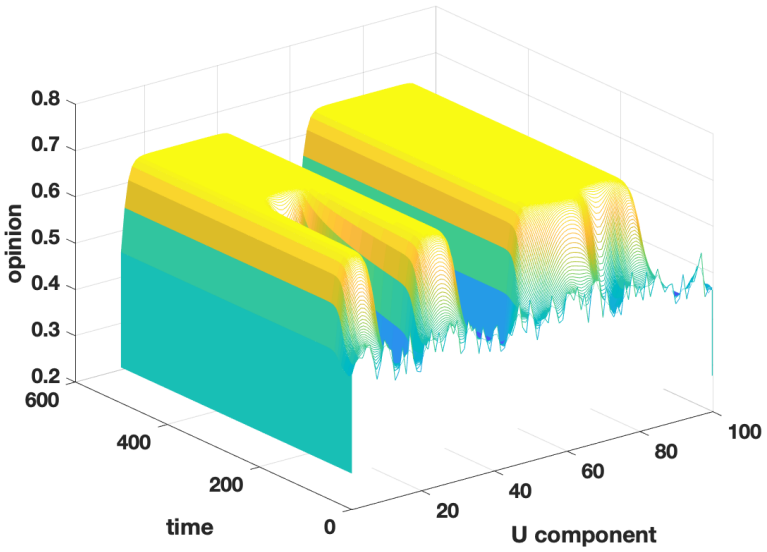

Figure 7: As in Figure 6 with initial condition sampled from $U(0.4, 0.6)$.

defined to be the first step at which the relative normwise difference between successive iterates does not exceed 10^{-8}, or $10,000$ if this value is smaller. On the right in Figure 11 we show how much movement each node underwent by computing the sample average of the vacillation, defined as

$$\frac{1}{\text{final}} \sum_{k=1}^{\text{final}-1} \|\mathbf{u}^{k+1} - \mathbf{u}^k\|_1, \tag{16}$$

where $\|\cdot\|_1$ denotes the 1-norm. (The standard errors in the two plots are negligible to visual accuracy.) We see that the mean time to steady state decays as as the rewiring probability is increased, while the vacillation grows. Intuitively, because our initial condition contains a region close to u_1 and a region close to u_2, when the connections are lattice-like (p small) each of these two states locally attracts a group of nodes—the system takes a long time to resolve the competition between the two states, but individual nodes spend a long time close to a single state. As we increase randomness in the connections (p large), the smoothness of the initial condition becomes less relevant— strong, like-minded and slow-moving clusters cannot survive over

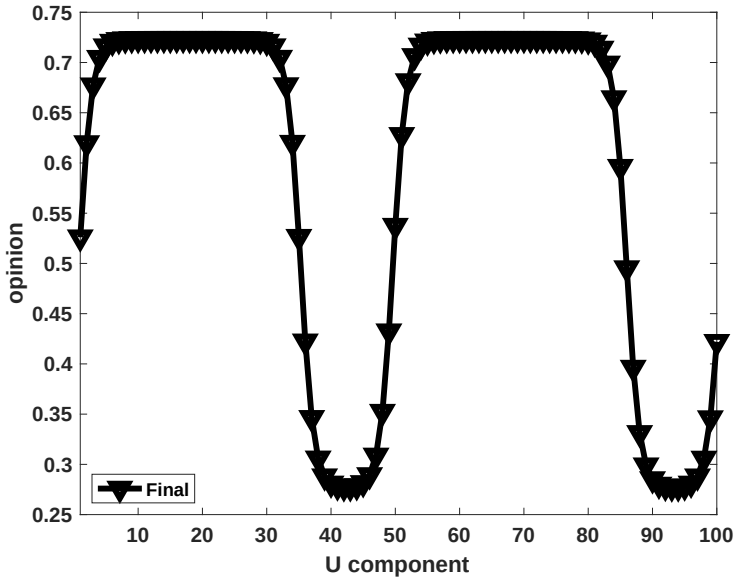

Figure 8: Profile after 500 steps from the computation in Figure 7.

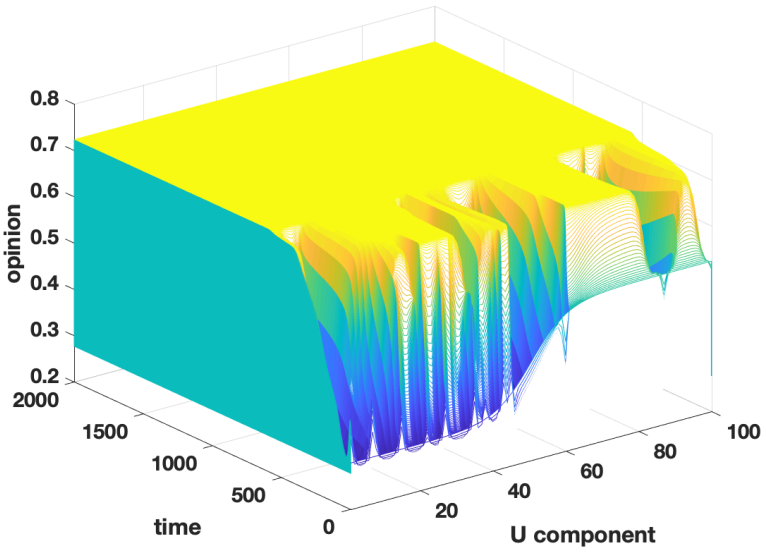

Figure 9: Evolution of opinions from a rewired periodic ring.

long time scales, so there is more rapid and dynamic evolution to steady state. In both cases, the variance drops dramatically with increasing p.

We note in passing that [18] identified a *small world* regime for intermediate p values where local clustering has not been destroyed, but the added shortcuts have reduced the typical pathlength. In our setting, it appears that this regime also combines the two properties of (a) rapid progress to steady state, and (b) gradual changes in opinion profiles.

5.2 Preferential Attachment

We finish by considering the case where A is a sample from the preferential attachment model of [4]. The upper picture in Figure 12 shows the nonzero structure in the adjacency matrix. Here $n = 100$ and the network sample was computed with the `pref.m` function from [17], using the default parameters. The lower plot shows the degree of each node. We see that node 1 has the highest degree, and, more generally, lower indexed nodes have higher degrees.

For the same r, θ and ϵ values as in the previous experiments, the upper plot in Figure 13 shows the evolution of opinions in the case where the initial

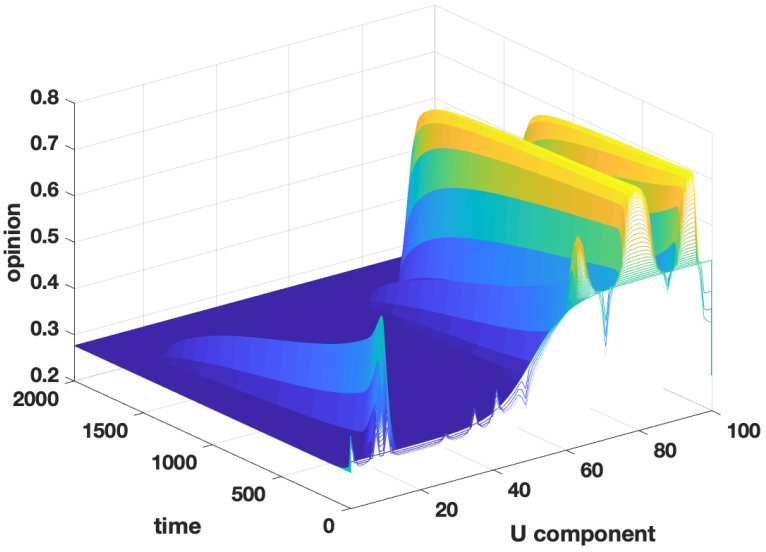

Figure 10: Same parameters as in in Figure 9 with a different random choice of rewiring.

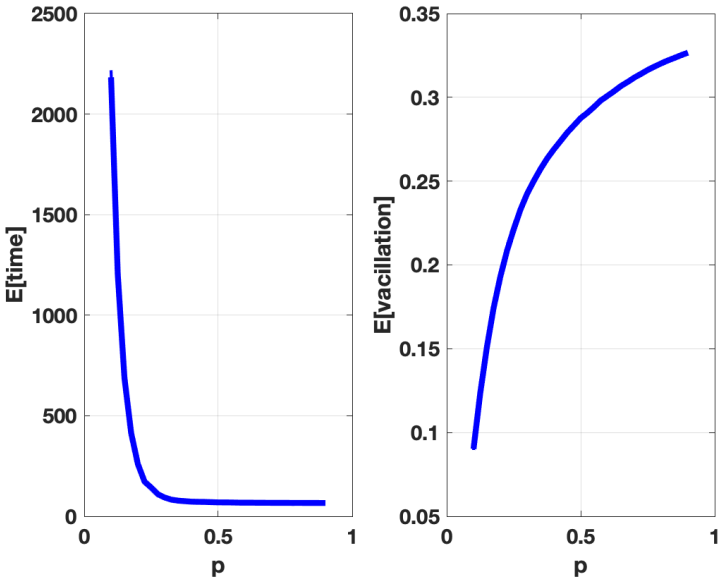

Figure 11: Solution characteristics as the rewiring parameter, p, is varied (horizontal axis). Left: mean number of steps until solutions appears to reach steady state. Right: variation in the solution over time, as defined in (16).

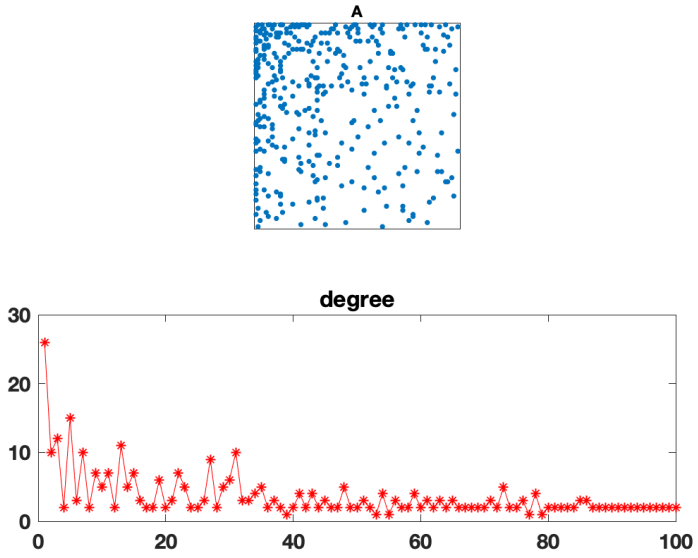

Figure 12: Upper: adjacency matrix from a preferential attachment model. Lower: nodal degrees.

condition has the form $u_i^0 = 0.1$ for $i = 1, 2, \ldots, 21$ and $u_0^i = 0.8$ for $i = 22, 23, \ldots, 100$. Here, the first 21 nodes, which include all those of high degree, are given initial conditions close to the lower steady state value, u_1. The remaining 79 nodes start close to the upper steady state value, u_2. We see that the dynamics are dominated by the initial opinion shared by the larger set of nodes, and the system evolves towards the u_2 level. In the lower picture, we alter the initial condition so that $u_{22}^0 = 0.1$; adding one more node to the u_1 set. In this case, despite their numerical disadvantage, the high degree nodes are now able to dominate, and the system is attracted to the u_1 level.

6 Conclusions

In this work we developed and analyzed a network-based model that incorporates the *unthinking/confident extremists* or *rigidity-of-the-extreme* effects [6, 19], and was motivated by the stochastic differential equation model of

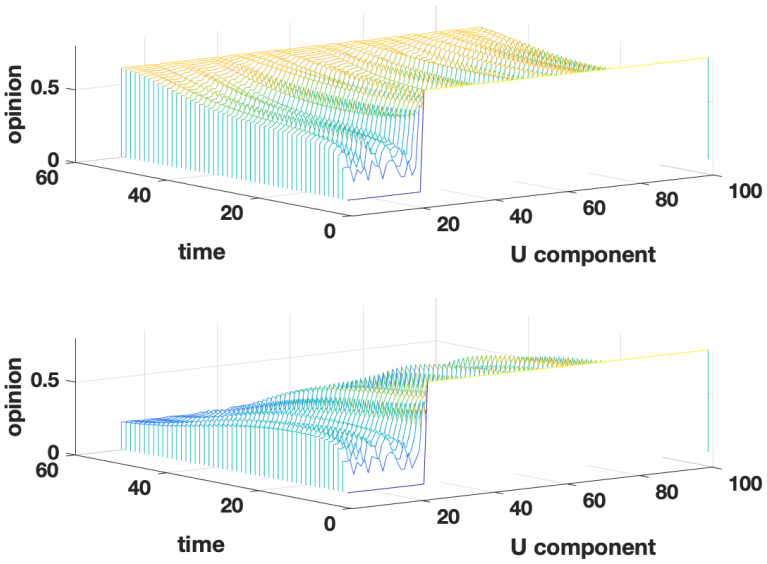

Figure 13: Evolution of the system with adjacency matrix from Figure 12 for two different initial conditions that differ only for node 22.

Cobb [7].

Analysis shows that the model can support two distinct stable steady states and, moreover, the system may spend a significant amount of time with an opinion profile that contains patches of extreme views from each end of the one-dimensional political spectrum. Indeed, up to the accuracy of floating point arithmetic, these highly polarized profiles are effectively steady state solutions. A further consequence of the bi-stability in the model is that the equilibrium behavior of the system can be extremely sensitive to microscale details: subtle changes to the initial profile or the local connectivity pattern can cause qualitatively different long-term results. We also saw that, in the case of randomized connectivity, where an initial condition that is "smooth" with respect to the component index no longer corresponds to like-minded neighbors, there can be rapid transitions as smaller patches compete and subsume or become subsumed.

There are many interesting directions in which this work could be developed. These include

- testing the model on further network classes,
- analysing the nature of the transitions between extreme levels in the "quasi-steady-state" solutions, as, for example, in Figure 8,
- fitting the model to relevant data sets,
- extending the model to allow the network topology to evolve alongside the opinion profile, and
- developing and testing analogous agent based models where individuals who hold more extreme opinions are less likely to be influenced by their associates.

References

[1] Giacomo Albi, Lorenzo Pareschi, Giuseppe Toscani, and Mattia Zanella. Recent advances in opinion modeling: Control and social influence. *Active Particles*, 1:49–98, 2017.

[2] Brian D. O. Anderson and Mengbin Ye. Recent advances in the modelling and analysis of opinion dynamics on influence networks. *International Journal of Automation and Computing*, 16:129–149, 2019.

[3] Robert Axelrod. The dissemination of culture: A model with local convergence and global polarization. *Journal of Conflict Resolution*, 41:203–226, 1997.

[4] A. L. Barabási and R. Albert. Emergence of scaling in random networks. *Science*, 286(5439):509–512, 1999.

[5] V. D. Blondel, J. M. Hendrickx, and J. N. Tsitsiklis. On Krause's multi-agent consensus model with state-dependent connectivity. *IEEE Transactions on Automatic Control*, 54:.2586–2597, 2009.

[6] Mark J. Brandt, Anthony M. Evans, and Jarret T. Crawford. The unthinking or confident extremist? Political extremists are more likely than moderates to reject experimenter-generated anchors. *Psychological Science*, 26(2):189–202, 2015.

[7] Loren Cobb. Stochastic differential equations for the social sciences. In Loren Cobb and Robert M. Thrall, editors, *Mathematical Frontiers of the Social and Policy Sciences*. Westview Press, 1981.

[8] M. H. DeGroot. Reaching a consensus. *J. Am. Stat. Assoc.*, 69:118–121, 1974.

[9] Noah E. Friedkin and Eugene C. Johnsen. Social influence and opinions. *The Journal of Mathematical Sociology*, 15:193–206, 1990.

[10] Hu Haibo. Competing opinion diffusion on social networks. *Royal Society Open Science*, 4:171160, 2017.

[11] Desmond J. Higham. An algorithmic introduction to numerical simulation of stochastic differential equations. *SIAM Review*, 43:525–546, 2001.

[12] Fima C. Klebaner. *Introduction to Stochastic Calculus with Applications*. Imperial College Press, London, 1998.

[13] Peter E. Kloeden and Eckhard Platen. *Numerical Solution of Stochastic Differential Equations*. Springer-Verlag, Berlin, 1992.

[14] James D. Murray. *Mathematical Biology I. An Introduction*, volume 17 of *Interdisciplinary Applied Mathematics*. Springer, New York, 3 edition, 2002.

[15] Nicola Perra and Luis E. C. Rocha. Modelling opinion dynamics in the age of algorithmic personalisation. *Scientific Reports*, 9:7261, 2019.

[16] Hegselmann R. and Krause U. Opinion dynamics and bounded confidence: models, analysis, and simulation. *J. Artif. Soc. Soc. Simul.*, 5, 2002.

[17] Alan Taylor and Desmond J. Higham. CONTEST: A controllable test matrix toolbox for MATLAB. *ACM Trans. Math. Softw.*, 35(4):26:1–26:17, 2009.

[18] D. J. Watts and S. H. Strogatz. Collective dynamics of 'small-world' networks. *Nature*, 393:440–442, 1998.

[19] Leor Zmigrod, Peter J. Rentfrow, and T. W. Robbins. The partisan mind: Is extreme political partisanship related to cognitive inflexibility? *Journal of Experimental Psychology. General*, page online first, 2019.